Energy Detection for M-QAM Signals

Shun Ishihara*, Kenta Umebayashi**
Faculty of Engineering
Tokyo University of Agriculture and Technology
Tokyo, Japan
ishihara1405@st.go.tuat.ac.jp*
ume_k@cc.tuat.ac.jp**

Janne Lehtomäki
Centre for Wireless Communications
University of Oulu
Oulu, Finland
janne.lehtomaki@oulu.fi

***Abstract*—In this paper, we address energy detection for M-ary quadrature amplitude modulation (QAM) signals. In the literature deterministic signal model is widely used and detection probability is a function of signal energy. Unlike constant amplitude signals, the QAM signal is not deterministic since the energy in each QAM symbol can randomly vary. For random signals, model where both signal and noise are Gaussian has been widely used. However, this approximation may not provide accurate detection probability for QAM signals. Instead the detection probability should be averaged over the distribution of the energy. Previous work has considered calculating exact detection probability for given M analytically. However, the method presented previously has complexity that increases as a function of M and the number of samples.**

In this paper, we show that the distribution of observed energy for any M can be accurately approximated by one distribution which is derived analytically. Multiple numerical results showing probability density function, Kolmogorov-Smirnov distance, and detection probability are shown. Based on these results, a range where the proposed approximation is applicable is obtained.

***Index Terms*—Energy Detection, Quadrature Amplitude Modulation, Spectrum Sensing**

I. Introduction

The rapid increase in wireless communication services leads to the scarcity of spectrum resource for new wireless services/systems. The spectrum resource is usually allocated to each wireless services/systems exclusively and new wireless services/systems have difficulty in getting spectrum resource anymore [1]. However, according to numerous spectrum usage measurement campaigns, e.g. [2], utilization ratio of the allocated spectrum resource is not always high. This fact indicates that the spectrum resource has not been utilized efficiently.

In order to solve the spectrum scarcity problem, the concept of dynamic spectrum access (DSA) has emerged [3]. In the DSA concept, the un-licensed users, i.e. secondary users (SUs), can access the unused spectrum owned by licensed users, i.e. primary users (PUs), provided that the spectrum usage by the SU does not cause harmful interference to PU.

This work was supported by the European Commission in the framework of the H2020-EUJ-02-2018 project 5GEnhance (Grant agreement no. 815056), by "Strategic Information and Communications R&D Promotion Programme (SCOPE)" of Ministry of Internal Affairs and Communications (MIC) of Japan (Grant no. JPJ000595), the JSPS KAKENHI Grant Numbers JP18K04124 and JP18KK0109, and Institute of Global Innovation Research in TUAT. The work of J. Lehtomäki was supported by the Academy of Finland 6Genesis Flagship.

One way for the DSA to work is that SUs find unused spectrum where PU user is currently not transmitting. One possible way to find the unused spectrum is spectrum sensing which can detect whether the spectrum is used or not [4]. Energy detection (ED) is one of the most common methods for spectrum sensing. The benefits of ED include low complexity in terms of operation and implementation. Also it does not need a priori information about the received signal unlike for example matched filter based spectrum sensing.

For the design of ED, it is necessary to get statistics of observed energy which consists of a signal component and a noise component. Specifically, the detection threshold can be calculated based on the statistical distribution of observed energy. Typically, the noise component is assumed to follow a Gaussian distribution and the observed energy with only noise component follows the central Chi-square distribution. On the other hand, the signal component can belong to two categories: a deterministic signal or a random signal. In case of constant envelope modulation signal, such as M-ary phase shift keying (PSK) modulation using single-carrier technique, the energy of the signal component can be approximated by constant value and this corresponds to the deterministic category. In this case, the observed energy follows the non-central Chi-square distribution. For the random case, a simple method is to assume that the signal component follows Gaussian distribution [5]. An observed energy with a quadrature amplitude modulation (QAM) signal based on single-carrier technique belongs to the random case. However, the Gaussian approximation is not applicable. For this issue, a design for ED in the case of QAM signal based on single-carrier technique has been investigated in [6]. Specifically, analysis of ED performance has been shown and the analytical result depends on the number of signal points (M) of M-ary QAM and the number of received samples K. The analytical method in [6] can provide accurate analytical result. However it requires huge computational complexity when K and M are large.

In this paper, we investigate a simplified analytical derivation of the distribution of observed energy for the QAM signal case. The contributions of the paper are summarized as follow.

- We propose a method for approximating the distribution of observed energy for the QAM signal case. A remarkable thing is that the proposed method can provide the analytical distribution without depending on M.

- In the proposed method, we approximate finite M as infinity for low complexity. Although it is using an approximation, this method can give good accuracy even when M is small, such as $M = 16$.
- Numerical evaluations show the benefits of the proposed method in terms of accuracy as compared to a conventional method in the literature.

II. Energy detection

An assumed detection problem in the spectrum sensing is a binary hypothesis testing problem: $\mathcal{H}_0$ (only noise present) or $\mathcal{H}_1$ (noise and signal both present) as [7]:

$$\begin{aligned} &\mathcal{H}_0 : y[k] = w[k] \qquad && k = 0, 1, 2, ..., K-1 \\ &\mathcal{H}_1 : y[k] = \sqrt{P}x[k] + w[k] \qquad && k = 0, 1, 2, ..., K-1, \end{aligned} \tag{1}$$

where k is the index number for the time domain sample, K is the number of samples during the observation interval, $y[k]$ is an observed signal at the SU, $w[k]$ is noise component which follows circularly symmetric zero mean complex Gaussian distribution with zero mean and variance σ_n^2, $x[k]$ is a signal component sent from the PU with unit variance, and P indicates the average power for the signal component. The noise component is uncorrelated with $x[k]$. The assumed modulation type for $x[k]$ is M-ary QAM where M is power of two, such as 16, 64 and 256. Since the observed energy is not affected by frequency and phase offsets, they are not considered in this paper [8].

The normalized observed energy $V^{'}$ at the SU is given by:

$$\mathcal{H}_0 : V^{'} = \sum_{k=0}^{K-1} \left(\frac{w_{\mathrm{I}}[k]}{\frac{\sigma_n}{\sqrt{2}}} \right)^2 + \sum_{k=0}^{K-1} \left(\frac{w_{\mathrm{Q}}[k]}{\frac{\sigma_n}{\sqrt{2}}} \right)^2 \tag{2}$$

$$\begin{aligned} \mathcal{H}_1 : V^{'} = &\sum_{k=0}^{K-1} \left(\frac{\sqrt{P}x_{\mathrm{I}}[k] + w_{\mathrm{I}}[k]}{\frac{\sigma_n}{\sqrt{2}}} \right)^2 \\ &+ \sum_{k=0}^{K-1} \left(\frac{\sqrt{P}x_{\mathrm{Q}}[k] + w_{\mathrm{Q}}[k]}{\frac{\sigma_n}{\sqrt{2}}} \right)^2, \end{aligned} \tag{3}$$

where I and Q indicate inphase and quadrature component of $x[k]$ and $w[k]$, respectively. The observed energy is normalized by $\sigma_n^2/2$ in (3) without loss of generality [6]. The detection rule is as follows: if $V^{'}$ is larger than the predetermined threshold $V_T^{'}$, the detection result is $\mathcal{H}_1$, otherwise the detection result is $\mathcal{H}_0$, i.e.

$$V^{'} \underset{\mathcal{H}_0}{\overset{\mathcal{H}_1}{\gtrless}} V_T^{'}. \tag{4}$$

Two criteria to express performance of ED are the false alarm probability (P_{FA}) and the detection probability (P_D). The event for P_{FA} is that the detection result is $\mathcal{H}_1$ when $\mathcal{H}_0$ is correct hypothesis and the event for P_D is that the detection result is $\mathcal{H}_1$ when $\mathcal{H}_1$ is the correct hypothesis. Mathematically P_{FA} and P_D are given by:

$$P_{FA} = \Pr(V^{'} \geq V_T^{'} | \mathcal{H}_0) \tag{5}$$

$$P_D = \Pr(V^{'} \geq V_T^{'} | \mathcal{H}_1), \tag{6}$$

where $\Pr()$ is the probability of its argument. The average signal to noise power ratio (SNR) is defined by $\gamma = P/\sigma_n^2$. The detection probability depends on the average SNR, $V_T^{'}$ and possible randomness in the signal (this is explained in the next Section).

III. Analytical design of ED

For designing ED properly, the threshold $V_T^{'}$ has to be set to satisfy either target P_{FA} or P_D.

For satisfying the target P_{FA}, we need to know statistics of $V^{'}$ under $\mathcal{H}_0$. It is well known that the probability density function (PDF) of $V^{'}$ under $\mathcal{H}_0$ follows a central chi-square distribution with $2K$ degrees of freedom (DOF) [9], and the distribution is given by

$$p(V^{'}|\mathcal{H}_0) = p_{\chi^2,K}(V^{'}) = \begin{cases} \dfrac{V^{'K-1} e^{-\frac{V^{'}}{2}}}{2^K \Gamma(K)} & V^{'} > 0 \\ 0 & otherwise \end{cases} \tag{7}$$

where $\Gamma(K)$ is the gamma function.

On the other hand, P_D depends on $V^{'}$ under $\mathcal{H}_1$. Let λ denote the normalized observed energy due to signal component in $V^{'}$ and λ is defined by

$$\lambda = \sum_{k=0}^{K-1} \left(\frac{\sqrt{P}x_{\mathrm{I}}[k]}{\frac{\sigma_n}{\sqrt{2}}} \right)^2 + \sum_{k=0}^{K-1} \left(\frac{\sqrt{P}x_{\mathrm{Q}}[k]}{\frac{\sigma_n}{\sqrt{2}}} \right)^2. \tag{8}$$

If the observed energy for the signal component λ is deterministic (such as for PSK since all its constellation symbols have the same energy), PDF of $V^{'}$ under $\mathcal{H}_1$ follows a noncentral chi-square distribution with $2K$ DOF as

$$p(V^{'}|\mathcal{H}_1) = p_{\chi^2,K}(V^{'}|\lambda) = \sum_{i=0}^{\infty} \frac{e^{\frac{-\lambda}{2}} (\frac{-\lambda}{2})^i}{i} p_{\chi^2,K}(V^{'}), \tag{9}$$

and λ is known as the non-centrality parameter in the chi-square distribution. In this case, an achievable P_D with a given threshold is [6]:

$$P_D = Q_K\left(\sqrt{\lambda}, \sqrt{V_T^{'}}\right), \tag{10}$$

where $Q_K(\cdot)$ is the generalized Marcum Q-function [10].

In the case where randomness in signal leads to the signal energy following a random distribution, λ may follow PDF $p(\lambda)$ and PDF of $p(V^{'}|H_1)$ is given by

$$p(V^{'}|H_1) = \int_0^{\infty} p_{\chi^2,K}(V^{'}|\lambda) p(\lambda) d\lambda. \tag{11}$$

Similarly, by averaging (10) over $p(\lambda)$, P_D can be obtained by [11]

$$P_D = \int_{V_T^{'}}^{\infty} p(V^{'}|H_1) dV^{'} = \int_0^{\infty} Q_K\left(\sqrt{\lambda}, \sqrt{V_T^{'}}\right) p(\lambda) d\lambda. \tag{12}$$

If there is a target P_D, $V^{'}$ has to be set properly to satisfy the target P_D and knowledge of distribution $p(V^{'}|H_1)$.

In a typical approach, it is assumed that signal component $x[k]$ follows Gaussian distribution and in this case $p(V^{'}|H_1)$

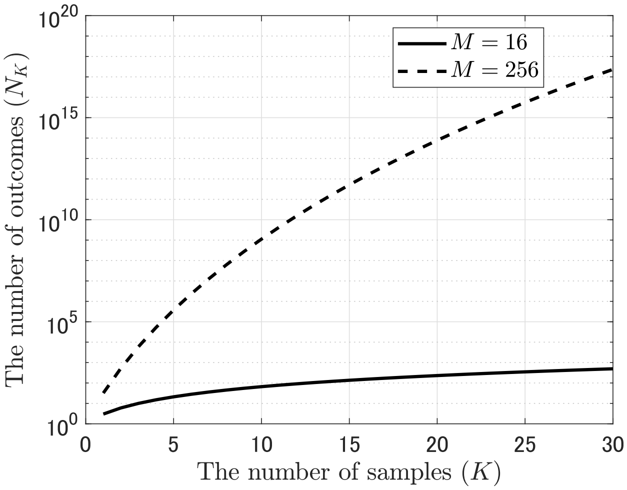

Fig. 1: The number of outcomes as a function of the number of samples

follows the generalized chi-squared distribution similarly to (7) [12]. This method is denoted by a conventional Gaussian approximation (CGA) in this paper.

The other conventional method and a proposed method to derive the distribution of ED output V' for M-QAM signal are shown as follows.

A. Exact solution (ES)

In [6], the distribution of observed energy due to signal component, λ, is attempted to be derived exactly. Let ${\mathbb{E}_{\mathbb{S}}}^K$ denote the sample space of observed energy contributed by signal component during K samples. In this case, the exact $p(\lambda)$ can be expressed by

$$p(\lambda) = \sum_{\epsilon \in {\mathbb{E}_{\mathbb{S}}}^K} \delta(\lambda - \epsilon)\mathrm{Pr}(\epsilon), \tag{13}$$

where $\mathrm{Pr}(\epsilon)$ denote probability of observed energy ϵ due to the signal components. Then, by using (12), P_D is given by

$$P_D = \sum_{\epsilon \in {\mathbb{E}_{\mathbb{S}}}^K} \mathrm{Pr}(\epsilon) Q_K(\sqrt{\lambda(\epsilon)}, \sqrt{V_T'}). \tag{14}$$

One issue in this method is that the number of elements in the set ${\mathbb{E}_{\mathbb{S}}}^K$ elements could be significantly large. Let us denote the number of elements in ${\mathbb{E}_{\mathbb{S}}}^K$ as N_K. It is given by [6]

$$N_K = \frac{(N_1 + K - 1)!}{(N_1 - 1)!K!}, \tag{15}$$

where N_1 depends on M. An example of N_K is shown in Fig. 1. Specifically, N_K as a function of K for $M = 16$ and $M = 256$ are plotted in Fig. 1. This figure indicates that even for $K = 30$, N_K can be a significantly large for large M. In [6], at most $K = 15$ with $M = 16$ was investigated and larger K and M may be difficult to handle.

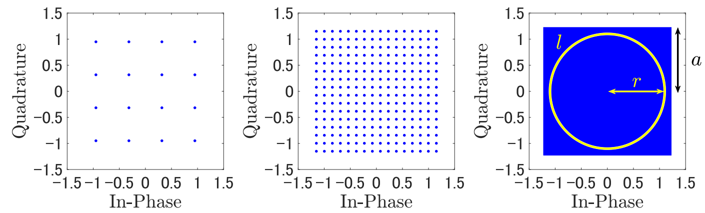

(a) $M = 16$ (b) $M = 256$ (c) $M = \infty$

Fig. 2: Constellation points for M-QAM.

B. Proposed method (PM)

In the proposed method, we employ $p(\lambda)$ with $M = \infty$ and this distribution corresponds to an approximated $p(\lambda)$ with finite number of M. In Fig. 2, constellation points for different M (16, 256, and ∞) are plotted. This figure shows that the distributions of $x[k]$ have a square shape. The PDF of λ with $K = 1$ and $M = \infty$ can be expressed by

$$p_{\infty,1}(\lambda) = \begin{cases} \dfrac{\pi}{8\gamma a^2} & (0 < \lambda \leq 2\gamma a^2) \\ \dfrac{\frac{\pi}{2} - 2\cos^{-1}\sqrt{\frac{2\gamma a^2}{\lambda}}}{4\gamma a^2} & (2\gamma a^2 \leq \lambda \leq 4\gamma a^2), \end{cases} \tag{16}$$

where suffix 1 of $p_{\infty,1}(\lambda)$ corresponds to $K = 1$ and $2a$ is one side of IQ plane ($a = \sqrt{\frac{3}{2}}$), as Fig. 2c shows. The details of the derivation of $p_{\infty,1}$ are shown in Appendix A. For the general K, $p_{\infty,K}(\lambda)$ can be obtained by

$$p_{\infty,K}(\lambda) = \overbrace{p_{\infty,1}(\lambda) * p_{\infty,1}(\lambda) \cdots p_{\infty,1}(\lambda)}^{K}, \tag{17}$$

where $*$ denotes convolution. By substituting $p_{\infty,K}(\lambda)$ for $p(\lambda)$ in (11), the approximated $p(V'|H_1)$ is available. One of benefits in PM is the the distribution does not depend on M. In case of adaptive modulation scheme such as IEEE Std 802.11ad-2012 [13], there are multiple QAM can be used and it is difficult to know which QAM is used in the observed signals.

IV. Simulation Results

In this section, we evaluate the approximated distributions based on CGA and PM to show the benefit of the proposed method by comparing with the Monte Carlo simulation based PDF with multiple M.

In Fig. 3, the approximated distributions based on CGA and PM, and Monte Carlo simulation based PDF of V' for $M = 16$, 64 and 256 are shown. In this evaluation, $K = 10$ and $\gamma = 0$ dB. Typically, ED for spectrum sensing is performed at such low SNR [4]. The remarkable thing is that PDFs of V' based on Monte Carlo simulations approximately coincide with the distribution with PM. In fact, the mean of V' does not depend on M and the variance of V' ($\sigma_{V'}^2$) as a function of M asymptotically approaches a certain value as [14]

$$\sigma_{V'}^2 = 4K\left(2\left(1 - \frac{1}{5}\frac{4M - 1}{M - 1}\right)\gamma^2 + 2\gamma + 1\right). \tag{18}$$

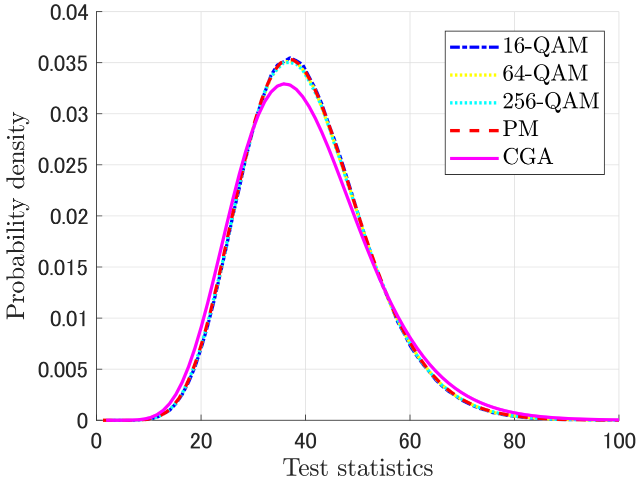

Fig. 3: PDF of observed energy for empirical distributions, PM and CGA with $\gamma = 0$ dB and $K = 10$

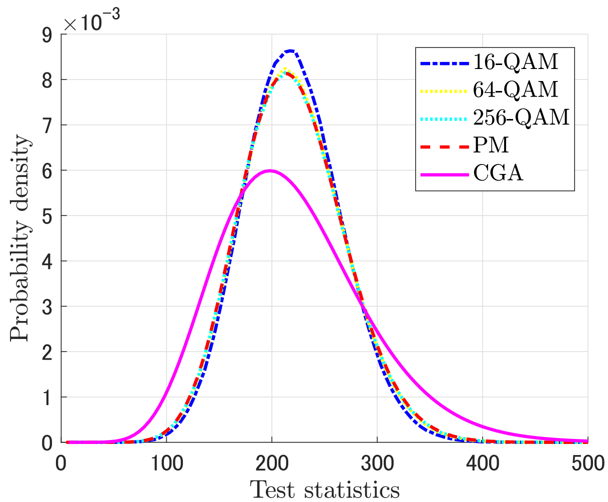

Fig. 4: PDF of observed energy for empirical distributions, PM and CGA with $\gamma = 10$ dB and $K = 10$

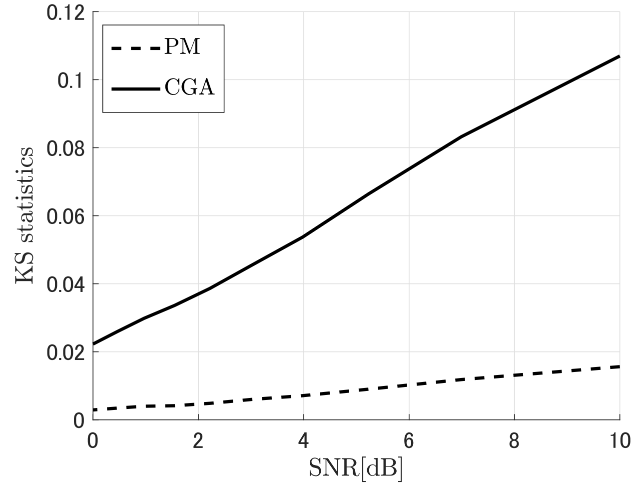

Fig. 5: KS statistics as a function of γ with $M = 16$ and $K = 10$

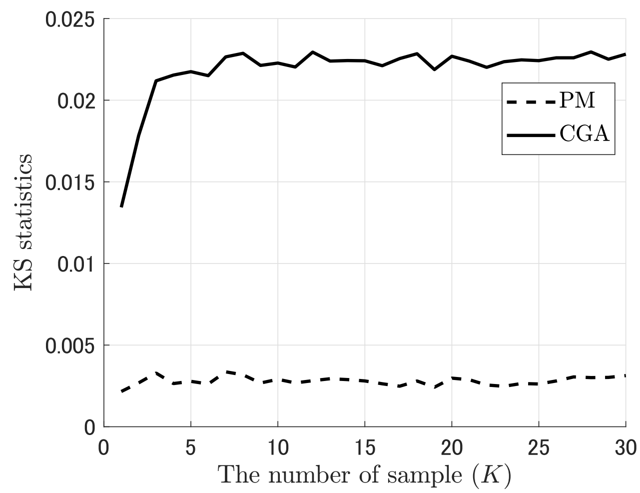

Fig. 6: KS statistics as a function of K with $M = 16$ and $\gamma = 0$ dB

It can be seen from the figure that the distribution obtained with PM coincides with the simulation results, showing its accuracy. On the other hand, there is a gap between the approximated distributions obtained by CGA and the empirical PDFs.

In Fig. 4, the PDFs obtained by the approximated distributions and empirical PDFs are shown. In this evaluation, $K = 10$ and $\gamma = 10$ dB. Therefore, this result corresponds to a high SNR case. The gap between distribution obtained by CGA and the other distributions has increased compared to the result in Fig. 3. In addition, the empirical distribution with $M = 16$ is also slightly different from the other empirical distributions. Thus, the approximated distributions based on the proposed method are more appropriate for higher values of M and/or low γ.

In order to evaluate the validity of the proposed method in different scenarios in terms of SNR, K and M, we employ Kolmogorov-Smirnov (KS) test [15] as Goodness-Of-Fit (GOF) metrics. In the KS statistic, a difference between empirical cumulative distribution function (CDF) and target CDF, such as approximated CDFs by CGA and PM, is used. Specifically, the KS statistic is defined by

$$D_{KS} = \max_{V'_{KS} < V' < \infty} |S(V') - P(V')|, \tag{19}$$

where V'_{KS} is used to determine a range for the CDF. Without loss of generality, V'_{KS} is set to satisfy $P(V'_{KS}) = 0.1$. The reason of $P(V'_{KS}) = 0.1$ is to evaluate the KS statistic in the region in terms of CDF where $P_D > 0.9$ according to the requirement of P_D in the IEEE 802.22 standard [16].

Fig. 5 shows KS statistics as a function of γ for $M = 16$ and $K = 10$. As confirmed in Figs. 3 and 4, increase of SNR

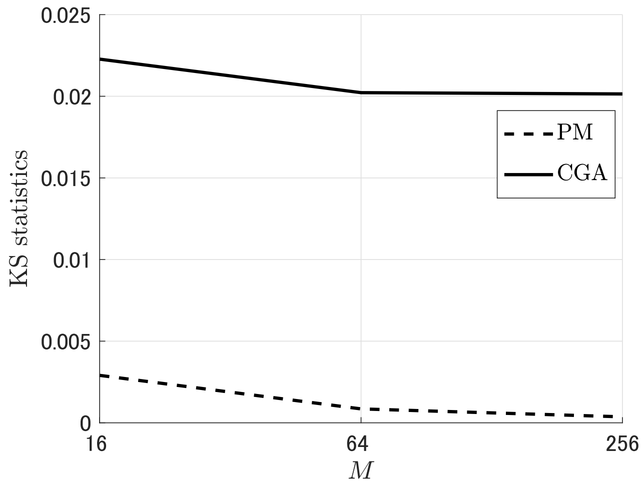

Fig. 7: KS statistics where $K = 10$ and $\gamma = 0$ dB

corresponds to increase in the KS statistic in CGA. On the other hand, the variation of SNR does not lead to significant changes in KS statistics of PM. The PM can achieve better accurate performance in any SNR than CGA.

Fig. 6 shows KS statistics as a function of K (number of samples) for $M = 16$ and $\gamma = 0$ dB. For PM and CGA the KS statistics are approximately constant in terms of K and PM can again achieve better accurate performance. In Fig. 7, KS statistics as a function of M for low SNR ($\gamma = 0$ dB) is shown. In all methods, higher number of M leads to more accurate performance.

V. Conclusion

For the design of ED with M-ary QAM modulation signals, we proposed an approximation in terms of PDF of observed energy at ED. In a previous work, an exact solution of PDF regarding the observed energy with M-ary QAM was used to design ED. However, this method leads to enormous computational complexity in case of large K and M. To address this issue, we approximate the PDF of the observed energy for all M by assuming $M = \infty$ and derive exact distribution for this assumption. Based on the numerical evaluations, we can confirm that the proposed method always exceeds the performance of that of the conventional method for random signal case (that assumes Gaussian signal).

Appendix A
Derivation of $p_{\infty,1}(\lambda)$ for PM

In the following, derivation of $p_{\infty,1}(\lambda)$ is shown. Fig.2c is IQ plane, where blue plane is aggregation of constellation points of $x[k]$ in $M = \infty$. Circumference l on blue plane is:

$$l = \begin{cases} 2\pi r & (0 < r \leq a) \\ 4r\left(\frac{\pi}{2} - 2\cos^{-1}\frac{a}{r}\right) & (a \leq r \leq \sqrt{2}a), \end{cases} \tag{20}$$

where r is radius as Fig. 2c shows. Since l can be interpreted as likelihood of r, $p_{\infty,1}(r)$ is given by:

$$p_{\infty,1}(r) = \begin{cases} \frac{\pi r}{2a^2} & (0 < r \leq a) \\ \frac{r}{a^2}\left(\frac{\pi}{2} - 2\cos^{-1}\frac{a}{r}\right) & (a \leq r \leq \sqrt{2}a), \end{cases} \tag{21}$$

where $p_{\infty,1}(r)$ can be calculated by the normalization of $4a^2$, the area of IQ plane. Moreover, since λ is described as $2\gamma r^2$ when $K = 1$, $p_{\infty,1}(\lambda)$ can be calculated by using the transformation of random variable from r to λ as follows:

$$p_{\infty,1}(\lambda) = \begin{cases} \frac{\pi}{8\gamma a^2} & (0 < \lambda \leq 2\gamma a^2) \\ \frac{\frac{\pi}{2} - 2\cos^{-1}\sqrt{\frac{2\gamma a^2}{\lambda}}}{4\gamma a^2} & (2\gamma a^2 \leq \lambda \leq 4\gamma a^2). \end{cases} \tag{22}$$

References

[1] G. Staple and K. Werbach, “The end of spectrum scarcity [spectrum allocation and utilization],” *IEEE Spectrum*, vol. 41, no. 3, pp. 48–52, 2004.

[2] FCC, “Spectrum policy task force report,” in *FCC, Tech. Rep. Docket*, no. 02-135, Nov 2002.

[3] I. F. Akyildiz, W.-Y. Lee, M. C. Vuran, and S. Mohanty, “Next generation/dynamic spectrum access/cognitive radio wireless networks: A survey,” *Computer networks*, vol. 50, no. 13, pp. 2127–2159, 2006.

[4] T. Yucek and H. Arslan, “A survey of spectrum sensing algorithms for cognitive radio applications,” *IEEE Communications Surveys Tutorials*, vol. 11, no. 1, pp. 116–130, First 2009.

[5] M. López-Benítez and F. Casadevall, “Improved energy detection spectrum sensing for cognitive radio,” *IET Communications*, vol. 6, no. 8, pp. 785–796, May 2012.

[6] D. S. Chaves and A. N. Barreto, “Energy detection spectrum sensing of M-ary QAM systems over AWGN channels,” in *2012 International Symposium on Wireless Communication Systems (ISWCS)*, Aug 2012, pp. 106–110.

[7] R. Umar, A. U. H. Sheikh, and M. Deriche, “Unveiling the hidden assumptions of energy detector based spectrum sensing for cognitive radios,” *IEEE Communications Surveys Tutorials*, vol. 16, no. 2, pp. 713–728, Second 2014.

[8] T. Cui, J. Tang, F. Gao, and C. Tellambura, “Moment-based parameter estimation and blind spectrum sensing for quadrature amplitude modulation,” *IEEE Transactions on Communications*, vol. 59, no. 2, pp. 613–623, February 2011.

[9] H. Urkowitz, “Energy detection of unknown deterministic signals,” *Proceedings of the IEEE*, vol. 55, no. 4, pp. 523–531, April 1967.

[10] A. Nuttall, “Some integrals involving the Q_M function (corresp.),” *IEEE Transactions on Information Theory*, vol. 21, no. 1, pp. 95–96, 1975.

[11] J. Ma, G. Y. Li, and B. H. Juang, “Signal processing in cognitive radio,” *Proceedings of the IEEE*, vol. 97, no. 5, pp. 805–823, May 2009.

[12] J. Ma, G. Zhao, and Y. Li, “Soft combination and detection for cooperative spectrum sensing in cognitive radio networks,” *IEEE Transactions on Wireless Communications*, vol. 7, no. 11, pp. 4502–4507, November 2008.

[13] “Ieee standard for information technology–telecommunications and information exchange between systems–local and metropolitan area networks–specific requirements-part 11: Wireless lan medium access control (mac) and physical layer (phy) specifications amendment 3: Enhancements for very high throughput in the 60 ghz band,” *IEEE Std 802.11ad-2012*, pp. 1–628, 2012.

[14] S. Tariq, A. Ghafoor, and S. Z. Farooq, “Analysis of joint multiband sensing-time m-qam signal detection in cognitive radios,” *ETRI Journal*, vol. 34, no. 6, pp. 892–899, 2012.

[15] W. H. Press, S. A. Teukolsky, W. T. Vetterling, and B. P. Flannery, *Numerical recipes 3rd edition: The art of scientific computing*. Cambridge university press, 2007.

[16] J. J. Lehtomaki, J. Vartiainen, M. Juntti, and H. Saarnisaari, “Spectrum sensing with forward methods,” in *MILCOM 2006-2006 IEEE Military Communications conference*. IEEE, 2006, pp. 1–7.